Communication-Efficient Online Detection of Network-Wide Anomalies

Ling Huang[*] XuanLong Nguyen[*] Minos Garofalakis[†] Joseph Hellerstein[*]
Michael Jordan[*] Anthony D. Joseph[*] Nina Taft[†]
[*]UC Berkeley [†]Intel Research Berkeley
{hling, xuanlong, hellerstein, jordan, adj}@cs.berkeley.edu {minos.garofalakis, nina.taft}@intel.com

Abstract— **There has been growing interest in building large-scale distributed monitoring systems for sensor, enterprise, and ISP networks. Recent work has proposed using Principal Component Analysis (PCA) over global traffic-matrix statistics to effectively isolate network-wide anomalies. We propose a novel approximation scheme for online, distributed, PCA-based anomaly detection that dramatically reduces the burden on the production network. Our algorithm leverages intelligent data filtering at local monitors and analytical results based on stochastic matrix perturbation theory to effectively balance the tradeoff between detection accuracy and the amount of data communicated over the network. By avoiding the expensive step of centralizing all traffic data, our solution enables tracking PCA-based anomalies in real time with minimal data communications – this overcomes the key scalability limitations of the state-of-the-art network-wide anomaly detection solution. Experiments with traffic data from an ISP-backbone network demonstrate that our methods yield significant communication benefits while simultaneously achieving high detection accuracy.**

I. Introduction

Today's large distributed systems (e.g., server clusters, large Internet Service Provider (ISP), and enterprise networks) employ distributed monitoring infrastructures to collect and aggregate information describing system status and performance. Remote monitor sensors are typically deployed throughout the network yielding numerous large and widely-distributed time-series data streams representing information from multiple vantage points; this information is continuously monitored and analyzed for a variety of purposes.

An example application that employs a distributed monitoring infrastructure is one that seeks to detect network-wide traffic anomalies. Recent work by Lakhina, *et al.* [15] proposes an anomaly detection scheme in which monitors ship observations to a central Network Operations Center (NOC), which in turn assembles and analyzes the data to perform anomaly detection. Specifically, they propose that local monitors continuously measure the total volume of traffic (in bytes) on each network link, and periodically push all recent measurements to the NOC. The NOC then performs Principal Component Analysis (PCA) on the assembled data matrix to reveal traffic anomalies that were not detectable in any single link-level measurements. Lakhina, *et al.* demonstrate that this technique is quite effective in detecting anomalies in traffic, in part due to the inherently low-dimensional nature of the underlying data.

However, such a "periodic push" approach suffers from scalability limitations. There are two aspects to scalability: allowing the system to perform in real-time and without inducing congestion both as the number of monitors grows, and as the time scales at which detection operates shrinks. The work in [15] was initially shown to work at 5 or 10 minute time scales. Since many anomalies occur on much smaller time scales, if the method were employed on a second or sub-second time scale, then the volume of measurement data transmitted through the network would increase dramatically. Coupling this with an order of magnitude (or more) increase in monitors could lead to a explosion in the volume of data collection.

An approach in which *all* monitors upload *all* of their data to a central processing site regularly, creates two problems. First it may overload the central processing site. Second, sending such large quantities of data through the network is a problem for certain kinds of networks such as sensor networks and enterprise networks (that do not overprovision inter-site connectivity). Although such measurement overhead may be supportable in today's ISPs, it may not in the future as we move toward petascale monitoring infrastructures that will monitor hundreds or thousands of network data features.

It is a central premise of this work that backhauling all distributed monitoring data may be unnecessary, depending upon the particular monitoring task, and thus smart data-filtering or data-reduction at the local monitoring sites should be employed. This approach would enable distributed monitoring systems to scale more gracefully both as the number of monitors increase and as the time scale for data collection and anomaly detection decreases. The promising effectiveness of [15] provides strong motivation for designing a significantly more communication-efficient PCA-based scheme for real-time anomaly detection. We need viable solutions that process data "in-network" to intelligently control the frequency and size of monitoring data communications.

We are thus motivated to study how well traffic anomalies can be detected if only a portion of the monitored data is shipped to the NOC (often referred to as a *coordinator* hereafter). In this paper, we take the ideas of Lakhina, *et al.* and recast them in a communication-efficient framework that detects anomalies at a desired accuracy level with minimal communication cost. To do this, we leverage the monitors in *local* filtering (i.e., based on feedback from the NOC, they decide how much and when to send data to the NOC), while ensuring that the triggering condition for anomaly detection is based on the *global* data.

Our Contributions. We propose a novel approach for communication-efficient online detection of network-wide traffic anomalies. Our proposed solution is unusual in that it combines the existing PCA-based method with in-network processing ideas [5], [18] with new insights based on *Stochastic Matrix Perturbation (SMP) theory*. We develop an approximation technique in order to reduce the amount of data needed for anomaly detection. Having incomplete monitoring data, can lead to errors that propagate through the computation (including for example the computation of eigenvalues and anomaly trigger thresholds - all of which are data-driven). This results in an anomaly detector that can make mistakes. We make use of SMP theory to derive analytic bounds on each of the terms affected by error propagation. We design an algorithm that derives filtering parameters for the monitors, such that the errors made by the detector are bounded. Our algorithms allows users to input a target error rate which gives them control over the tradeoff between communication cost and detection accuracy.

Our evaluation using real-world data streams collected from a well known ISP network shows that our methods work very well. While sending less than 10% of the original time-series data (over an order of magnitude communication reduction), we guarantee that the detection error would be no more than 4% bigger than when using full data. In fact, our system performs much better than these bounds; we find that the actual error rates are nearly indistinguishable from the full-data method. This results in a huge savings in communication overhead (e.g., typically 80 or 90% of the original data is no longer sent) with only a very small impact on errors. Put another way, within the same (fixed) communication budget, our algorithms can allow for a ten-fold increase in the time granularity of network-statistics collection. Interestingly, we found that our method with filtered data does not inject any bias into the statistical tension between the underlying distributions of normal and abnormal traffic. Finally, we show that our system can indeed scale gracefully as the number of monitors grows.

Prior Work. A number of techniques have been proposed to detect network traffic anomalies [1], [4], [15], [22], [27]. Among them, Lakhina *et al.* [15], carried out pioneering work in detecting network-wide anomalies; Zhang *et al.* [27], extended it further and proposed a general "anomography" framework to infer network-level anomalies in both spatial and temporal domains. However, the goal of minimizing communication overhead in widely distributed Internet environments introduces new challenges. Recent progress in distributed monitoring, profiling and anomaly detection [19], [25], [26] aims to share information and foster collaboration between widely distributed monitoring boxes to offer improvements over isolated systems. These systems are examples for which a distributed detection tool such as ours would be useful.

In a distributed online setting, Keralapura *et al.* [14] proposed solutions to detect threshold violations on sum functions with specified accuracy while minimizing communication overhead. Sharfman *et al.* [21] proposed protocols to detect general distributed functions exceeding thresholds using a geometric decomposition method. However, their method assumes preset thresholds, does not consider global matrix analysis queries, and cannot scale to large networks with high-speed data streams. In a recent paper [8], we discussed some of the mathematical foundations of SMP theory and its application to distributed PCA tracking; here, we extend and strengthen these earlier mathematical results, and present novel techniques for casting our theoretical analyses in the context of a practical network anomaly detection system.

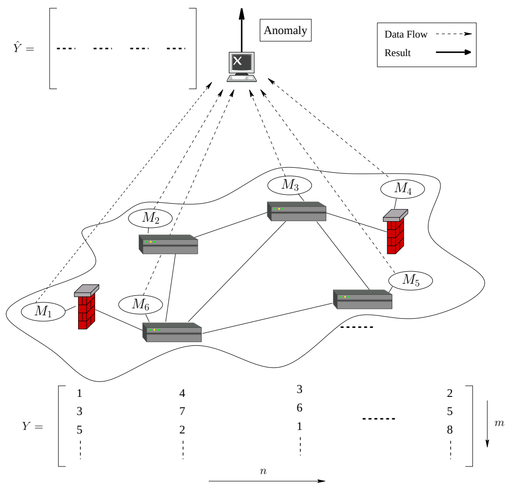

Fig. 1. The distributed monitoring system.

II. Problem description and background

We consider a monitoring system that includes a set of *distributed monitor nodes* $M_1, \ldots, M_n$, each of which collects a locally-observed time-series data stream (Fig. 1). For instance, the monitors may be attached to routers to collect the volume of traffic per second from each network link, participate in firewalls to log the number of TCP connection requests per second, or connect to servers to record the number of DNS transactions per minute. A central *coordinator node* seeks to observe the ensemble of these time series (i.e., the global network-wide data), and make global decisions such as those concerning matters of network-wide health[1]. The application of detecting *volume anomalies* across a large network employs such a distributed monitoring infrastructure. A volume anomaly refers to unusual traffic load levels in a network that are caused by anomalies such as DDoS attacks, flash crowds, device failures, misconfigurations, and so on.

Each monitor M_i collects a new data point $\mathbf{Y}_i(t)$ at every time step and, assuming a naive, "continuous push" protocol, sends the new point to the coordinator. Based on these updates, the coordinator keeps track of a sliding time window of size m (i.e., the m most recent data points) for each monitor's time

[1]There are several existing approaches [20] [28] that can be used to make our system avoid single point of failure. Regardless of the choice of fault-tolerance mechanism, our approach offers benefits and remains applicable.

series, organized into a matrix $\mathbf{Y}$ of size $m \times n$ (where the i^{th} column $\mathbf{Y}_i$ captures the data from monitor i, see Fig. 1). The coordinator then makes its decisions based on this global $\mathbf{Y}$ matrix.

Centralized Subspace Method for Volume Anomaly Detection. We now briefly summarize the PCA-based anomaly detector in [15]. As observed by Lakhina et al., due to the high level of traffic aggregation on ISP backbone links, volume anomalies can often go unnoticed by being "buried" within normal traffic patterns. On the other hand, they observe that, although, the measured data is of seemingly high dimensionality ($n =$ number of links), normal traffic patterns actually lie in a very low-dimensional subspace; furthermore, separating out this normal traffic subspace using PCA (to find the principal traffic components) makes it much easier to identify volume anomalies in the remaining subspace.

As before, let $\mathbf{Y}$ be the global $m \times n$ time-series data matrix, centered to have zero mean, and let $\mathbf{y} = \mathbf{y}(t)$ denote a n-dimensional vector of measurements (for all links) from a single time step t. Formally, PCA is a coordinate-transformation method that maps a given set of data points onto principal components ordered by the amount of data variance that they capture. The set of n principal components, $\{\mathbf{v}_i\}_{i=1}^n$, are defined as:

$$\mathbf{v}_i = \arg \max_{\|\mathbf{x}\|=1} \|(\mathbf{Y} - \sum_{j=1}^{i-1} \mathbf{Y}\mathbf{v}_j\mathbf{v}_j^T)\mathbf{x}\|$$

and are the n eigenvectors of the estimated covariance matrix $\mathbf{A} := \frac{1}{m}\mathbf{Y}^T\mathbf{Y}$. As shown in [15], PCA reveals that the Origin-Destination (OD) flow traffic matrices (i.e., the complete traffic demand across an entire network) of ISP backbones have low intrinsic dimensionality. Because the link traffic and the end-to-end traffic demands are linearly related, it turns out that the ensemble of all link traffic in a backbone network also exhibits low dimensionality. For example, in the Abilene network with 41 links, most data variance can be captured by the first $k = 4$ principal components. Thus, the underlying normal OD flows effectively reside in a (low) k-dimensional subspace of $\mathbb{R}^n$. This subspace is referred to as the *normal* traffic subspace $\mathcal{S}_n$. The remaining $(n - k)$ principal components constitute the *abnormal* traffic subspace $\mathcal{S}_a$.

Detecting volume anomalies relies on the decomposition of link traffic $\mathbf{y} = \mathbf{y}(t)$ at any time step into normal and abnormal components, $\mathbf{y} = \mathbf{y}_n + \mathbf{y}_a$, such that (a) $\mathbf{y}_n$ corresponds to modeled normal traffic (the projection of $\mathbf{y}$ onto $\mathcal{S}_n$), and (b) $\mathbf{y}_a$ corresponds to residual traffic (the projection of $\mathbf{y}$ onto $\mathcal{S}_a$). Mathematically, $\mathbf{y}_n(t)$ and $\mathbf{y}_a(t)$ can be computed as

$$\mathbf{y}_n(t) = \mathbf{P}\mathbf{P}^T\mathbf{y} = \mathbf{C}_n\mathbf{y} \text{ and } \mathbf{y}_a(t) = (\mathbf{I} - \mathbf{P}\mathbf{P}^T)\mathbf{y} = \mathbf{C}_a\mathbf{y}$$

where $\mathbf{P} = [\mathbf{v_1}, \mathbf{v_2}, \ldots, \mathbf{v_k}]$, is formed by the first k principal components which capture the dominant variance in the data. The matrix $\mathbf{C}_n = \mathbf{P}\mathbf{P}^T$ represents the linear operator that performs projection onto the normal subspace $\mathcal{S}_n$, and, $\mathbf{C}_a$ projects onto the abnormal subspace $\mathcal{S}_a$.

As observed in [15], a volume anomaly typically results in a large change to $\mathbf{y}_a$; thus, a useful metric for detecting abnormal traffic patterns is the squared prediction error (SPE): $\mathbf{SPE} \equiv \|\mathbf{y}_a\|^2 = \|\mathbf{C}_a\mathbf{y}\|^2$ More formally, their proposed algorithm signals a volume anomaly if

$$\mathbf{SPE} = \|\mathbf{C}_a\mathbf{y}\|^2 > Q_\alpha \tag{1}$$

where Q_α denotes the threshold statistic for the $\mathbf{SPE}$ residual function at the $1-\alpha$ confidence level. Such a statistical test for the $\mathbf{SPE}$ residual function, known as the Q-statistic [11], can be computed as a function $Q_\alpha = Q_\alpha(\lambda_{k+1}, \ldots, \lambda_n)$, of the $(n-k)$ non-principal eigenvalues of the covariance matrix $\mathbf{A}$. With the computed Q_α, this statistical test can guarantee that the false alarm probability is no more than α (under certain assumptions).

Our Communication Efficient Detection Problem. The problem we address is how to do the filtering at the monitors, so as to send as little data as possible through the network but still allow the anomaly detector to work accurately. The idea is that monitors should send a description of their time series signal, and then not send any more measurements (or summaries) until a change happens that is either ”sufficiently large” or likely to impact the global trigger condition being monitored. In our application, the trigger condition being monitored by the coordinator is that in Eqn (1). Because the monitors send data less frequently to the coordinator, the coordinator's view of the global network data can be out-of-date and perturbed. Thus, the statistics it computes for anomaly detection, such as the eigenvalues and projection matrix, will deviate from those of the true global state. This implies that the detection error at the coordinator (when triggering on condition (1)) will differ from that achieved using the full data.

Our solution includes the design of protocols used by the monitors and coordinator, and an algorithm to determine how to do the appropriate filtering. We allow the user (network operator) to input the tolerable *deviation μ of the false alarm probability*, a parameter that specifies how much the false alarm probability achieved by our approximation technique is permitted to deviate from the false alarm probability achieved by the centralized-data solution. We provide an algorithm for computing each monitor's filtering parameter that guarantees that our false alarm probability does not deviate by more than the specified deviation μ. In order to guarantee an error performance within μ, we need to track and limit the perturbations in the system caused by the local filtering at the monitors. This amounts to bounding the perturbations of the eigenvalues, projection matrix and trigger threshold (all of which get perturbed due to error propagation that occurs with out-dated measurement data). In this paper, we show that all of these system component errors can be bounded, and thus excellent detection can still be achieved, even with a substantial reduction in data transmitted to the coordinator.

Our filtering parameters are both heterogeneous (across different monitors) and adaptive in time. Intuitively, the selection of the filtering parameter at a monitor should take into account two things: the variability of the local time series data itself,

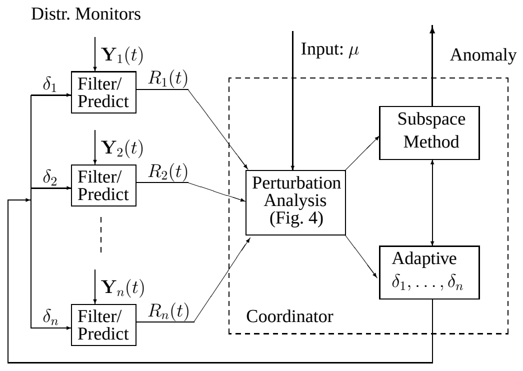

Fig. 2. Distributed detection system.

Symbol	Meaning
M_i	Monitor sites ($i = 1, \ldots, n$)
$\mathbf{Y}_i(t), \hat{\mathbf{Y}}_i(t)$	Data at monitor i and its approx. at the coordinator
$\mathbf{Y}, \hat{\mathbf{Y}}$	Data matrix at monitors and its approx. at the coordinator
$\mathbf{A}, \hat{\mathbf{A}}$	Cov. matrix at monitors and its approx. at the coordinator
$\lambda_i, \hat{\lambda}_i, \bar{\lambda}$	Eigenvalues of $\mathbf{A}$, $\hat{\mathbf{A}}$, and $\bar{\lambda} = \sum \hat{\lambda}_i/n$
$R_i(t)$	Most recent prediction model for $\mathbf{Y}_i(t)$
$\mathbf{W}_i(t), \mathbf{W}$	Filtering error time-series and matrix, $\mathbf{W} = \mathbf{Y} - \hat{\mathbf{Y}}$
$\mathbf{y}, \hat{\mathbf{y}}$	One time-step data from all monitors (one row of $\mathbf{Y}, \hat{\mathbf{Y}}$)
$\mathbf{C}_a, \hat{\mathbf{C}}_a$	The projection matrix of residual subspace
$\alpha, \hat{\alpha}$	False alarm (*i.e.*, false positive) probability
$Q_\alpha, \hat{Q}_\alpha$	The detection threshold
ϵ, ϵ^*	Tolerable and actual aggregate eigen-error
μ	Tolerable deviation of false alarm probability
δ, δ_i	Local monitor slack parameters

TABLE I
Notation.

and the marginal impact this particular data has on the global trigger condition relative to other data streams. We thus aim to do filtering locally at monitors using parameters that are derived based upon global correlations across different data streams and their joint impact on the trigger condition being tracked.

III. Our Approach

This section provides a description of several key elements of our novel approach to distributed detection. Our approach for distributed, PCA-based anomaly detection consists of two parts: (1) the monitors process their collected data by applying local filtering to suppress unnecessary message updates to the coordinator; and (2) the coordinator makes global decisions and provides feedback to the monitors (e.g., local filter parameter settings) based on the observed updates. The architecture of our system is depicted in Fig. 2.

As mentioned earlier, $\mathbf{Y}_i(t)$ denotes the actual time series observed at monitoring node M_i, which is one column vector of data matrix $\mathbf{Y}$. We use $R_i(t)$ to denote the approximate representation of $\mathbf{Y}_i(t)$ that is sent to the coordinator. If no further data is sent shortly after time t, the coordinator assumes that $R_i(t)$ serves as a *prediction* of the true data at these latter time instances. A simple prediction model might set $R_i(t)$ to the latest $\mathbf{Y}_i(t)$ value communicated from the site, or an average of recent communications, but more sophisticated prediction models [5], [12] can be used. Our techniques remain applicable regardless of prediction-model specifics.

The coordinator has two principal tasks: (1) to carry out anomaly detection, based on the PCA subspace method, using the inputs $R_i(t)$ it receives, and (2) to compute the filtering parameters δ_i for each monitor. The inputs to the coordinator are the false alarm rate deviation η, and the filtered time series. The outputs of the coordinator are a trigger that is fired whenever the condition in Eqn (1) is true, and the filtering parameters δ_i, that are sent to the monitors whenever they change. We also call the filtering parameter "slacks". The monitors use them by tracking the drift between the actual time series signal and the prediction function; whenever this drift exceeds the allowed slack, the monitor sends the coordinator an updated prediction, $R_i(t)$. Intuitively, these slacks are used to upper bound the difference between the coordinator's view of the data and the actual data.

The Local Monitor Protocol. Given a slack parameter δ_i, the protocol that runs at each monitor site M_i is fairly straightforward. Let $R_i(t)$ be the most recent prediction model for $\mathbf{Y}_i(t)$ sent to the coordinator. At any time t, monitor M_i continuously tracks the deviation of $\mathbf{Y}_i(t)$ from its prediction $R_i(t)$ as $\mathbf{W}_i(t) = \mathbf{Y}_i(t) - R_i(t)$, and checks the condition $|\mathbf{W}_i(t)| \leq \delta_i$ (*i.e.*, the monitor ensures that the absolute difference between its actual stream and the coordinator's corresponding prediction is upper bounded by its local slack δ_i. Whenever $|\mathbf{W}_i(t)| > \delta_i$, the monitor fires a local alarm and sends an update message to the coordinator that includes $\mathbf{Y}_i(t)$ and an up-to-date prediction $R_i(t)$, and resets $\mathbf{W}_i(t)$ to zero. (Table I summarizes our notation.)

The Coordinator Protocol. The coordinator maintains a perturbed version of the data matrix $\hat{\mathbf{Y}}$. The connection between the slacks and the coordinator's detection scheme comes from the following. The PCA at the coordinator is performed on a perturbed version of the covariance matrix, $\hat{\mathbf{A}} := \frac{1}{m}\hat{\mathbf{Y}}^T\hat{\mathbf{Y}} = \mathbf{A} + \mathbf{\Delta}$. The magnitude of the perturbation matrix $\mathbf{\Delta}$ is determined by the slack variables δ_i ($i = 1, \ldots, n$). We can thus bound the perturbation of the covariance matrix through the control of the slack variables.

The coordinator protocol works as follows. Each time t that a new input (from any monitor) arrives at the coordinator, it carries out the following steps:

1) Makes a new row of data $\hat{\mathbf{y}}$ as $\hat{\mathbf{y}} = [\ \hat{\mathbf{Y}}_1(t) \quad \hat{\mathbf{Y}}_2(t) \quad \ldots \quad \hat{\mathbf{Y}}_n(t)\ ]$, where $\hat{\mathbf{Y}}_i(t)$ is defined as either the update received from monitor i (if one exists), or the corresponding prediction $R_i(t)$ otherwise.
2) Updates its view of the global data $\hat{\mathbf{Y}}$, by replacing the oldest row of $\hat{\mathbf{Y}}$ using $\hat{\mathbf{y}}$.
3) Re-computes PCA on $\hat{\mathbf{Y}}$ using low-rank update algorithm. Then recompute the residual projection matrix $\hat{\mathbf{C}}_a$ and trigger threshold $\hat{Q}_\alpha$[2].

[2]Actually, it is not necessary to do this recomputation for every time step with new data coming in. A low-pass filtering condition on $\|\hat{\mathbf{A}}\|$ can dramatically reduce PCA-computation frequency without really sacrificing detection accuracy. Due to space constraints, the details are deferred to the full paper.

```
Procedure Monitor($i$, $\delta_i$)
Input: Monitor index $i$, local slack parameter $\delta_i$.
1.  while (true) do
2.      $t$ := current time
3.      $\mathbf{W}_i(t) := \mathbf{Y}_i(t) - R_i(t)$
4.      if ($|\mathbf{W}_i(t)| > \delta_i$) then
5.          Send update message $(i, \mathbf{Y}_i(t), R_i(t))$ to coordinator
6.          Set $\mathbf{W}_i(t) := 0$
7.      if (new slack $\delta_i^*$ is received from coordinator) then
8.          Set $\delta_i := \delta_i^*$

Procedure Coordinator($\mu$)
Input: Deviation $\mu$ on false alarm probability.
1.  while (true) do
2.      Make a new row of data $\hat{\mathbf{y}} = [\ R_1(t) \quad \ldots \quad R_n(t)\ ]$
3.      Replace the oldest row of $\hat{\mathbf{Y}}$ using $\hat{\mathbf{y}}$, pointed to by $\hat{\mathbf{Y}}_i(t)$
4.      for each (monitor update $(i, \mathbf{Y}_i(t), R_i^*(t))$ received) do
5.          Set local prediction $R_i(t) := R_i^*(t)$
6.          Set $\hat{\mathbf{Y}}_i(t) := \mathbf{Y}_i(t)$
7.      Re-compute PCA on $\hat{\mathbf{Y}}$ using low-rank update algorithm
8.      Re-compute threshold $\hat{Q}_\alpha$, matrix $\hat{\mathbf{C}}_a$ and residual $\|\hat{\mathbf{C}}_a\hat{\mathbf{y}}\|^2$
9.      if ( $\|\hat{\mathbf{C}}_a\hat{\mathbf{y}}\|^2 > \hat{Q}_\alpha$ ) then
            fire("anomaly"); break
10.     Compute new optimal settings for local slacks $\{\delta_i\}$ based on $\mu$
        and maintained statistics (Sec. IV)
11.     if (adaptive allocation) then  disseminate($\{\delta_i\}$)
```

Fig. 3. Procedures for (a) local monitor update processing, and (b) distributed detection at the coordinator.

4) Performs anomaly detection using $\hat{\mathbf{C}}_a, \hat{Q}_\alpha$ and $\hat{\mathbf{y}}$; fire an alarm if $\|\hat{\mathbf{C}}_a\hat{\mathbf{y}}\|^2 > \hat{Q}_\alpha$.

The coordinator can recompute the monitor slacks either periodically or upon each monitor update. The coordinator only sends new slacks to the monitors if there is a substantial change. Due to lack of space, we do not expand on this issue herein. A high-level pseudo-code description of both the local-monitor and coordinator protocols is depicted in Fig. 3.

IV. Parameter Design and Error Control

A key component of our framework is a practical method for choosing monitor slacks δ_i that effectively balance the tradeoff between the desirable loss of detection accuracy (i.e., due to the use of $\hat{\mathbf{Y}}$ instead of $\mathbf{Y}$) and the savings in data communication. Given an upper bound on the deviation μ of the false alarm probability from the (ideal) value α (guaranteed by the Q_α-statistic condition (1) in the centralized case), our goal is to determine δ_i values such the false alarm probability $\hat{\alpha}$ of our distributed detection protocol satisfies $\hat{\alpha} - \alpha < \mu$, while minimizing communication cost on the network [3].

To determine the δ_i values minimizing communication for a given μ, we need to be able quantify the effects of local monitor filtering on the observed false alarm probability. To this end, we appeal to *Stochastic Matrix Perturbation (SMP) theory* for quantifying the effects of the perturbation of a matrix on key quantities such as eigenvalues and eigen-subspaces, which in turn impact detection accuracy. Let λ_i and $\hat{\lambda}_i$ ($i = 1, \ldots, n$) denote the eigenvalues of the covariance

[3]Even though condition (1) is only a one-sided test, our experimental results demonstrate that our methods achieve very small missed-detection rates, similar to [15].

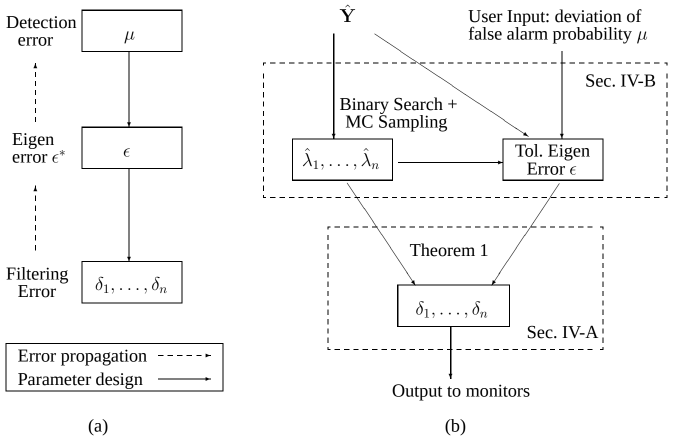
Detection error
μ
Eigen error ϵ^*
ϵ
Filtering Error
$\delta_1, \ldots, \delta_n$
Error propagation
Parameter design
(a)
$\hat{\mathbf{Y}}$
User Input: deviation of false alarm probability μ
Sec. IV-B
Binary Search + MC Sampling
$\hat{\lambda}_1, \ldots, \hat{\lambda}_n$
Tol. Eigen Error ϵ
Theorem 1
$\delta_1, \ldots, \delta_n$
Sec. IV-A
Output to monitors
(b)

Fig. 4. Perturbation analysis: from deviation of false alarm to monitor slacks.

matrix $\mathbf{A} = \frac{1}{m}\mathbf{Y}^T\mathbf{Y}$, and its perturbed version $\hat{\mathbf{A}} = \frac{1}{m}\hat{\mathbf{Y}}^T\hat{\mathbf{Y}}$. A key quantity in our methodology (serving as an intermediary between μ and the δ_i slacks) is the *L_2 aggregate eigen-error* ϵ^*, defined formally as $\epsilon^* := \sqrt{\frac{1}{n}\sum_{i=1}^n(\hat{\lambda}_i - \lambda_i)^2}$.

In a nutshell, the monitor slacks δ_i induce an eigen-error ϵ^* in the perturbed covariance matrix which, in turn, induces a false alarm probability deviation μ (Fig. 4(a)). Of course, in designing a practical anomaly-detection tool, our goal is to model error propagation in the *inverse* direction, moving from a desired false alarm deviation bound μ to monitor slacks δ_i that guarantee that bound while minimizing communication. This turns out to be a non-trivial task due to the complex dependencies across different parameters in our monitoring framework. In this section, we solve this problem of inverse error propagation in two steps, first demonstrating how to determine an upper bound on eigen-error ϵ^* given a false alarm deviation bound μ, and then showing how to determine "good" monitor slacks δ_i for a given eigen-error ϵ^* (Fig. 4(a)). Our presentation actually starts with the second step above, in order to introduce some basic concepts and ideas from SMP theory.

A. From tolerable eigen-error to monitor slacks

In our distributed protocol, the coordinator's view of the data matrix is the perturbed matrix $\hat{\mathbf{Y}} = \mathbf{Y} - \mathbf{W}$, where all elements of the column vector $\mathbf{W}_i$ are bounded within the interval $[-\delta_i, \delta_i]$. To keep the analysis tractable, we make the following assumptions on the filtering error matrix $\mathbf{W}$ (both fairly standard in SMP theory) :

1) The column vectors $\mathbf{W}_1, \ldots, \mathbf{W}_n$ are independent and radially symmetric m-dimensional vectors.
2) For each $i = 1, \ldots, n$, all elements of column vector $\mathbf{W}_i$ are i.i.d. random variables with mean 0 and variance $\sigma_i^2 := \sigma_i^2(\delta_i)$ (a function of the corresponding monitor slack).

Note that the independence assumption is on the single-monitor errors only – this by no means implies that the signals received by different monitors are statistically independent.

Let $\bar{\lambda} := \frac{1}{n}\sum\hat{\lambda}_i$ denote the average of the perturbed eigenvalues of $\hat{\mathbf{A}}$. Based on the statistical analysis on the

Frobenius norm of $\mathbf{\Delta}$, we can prove the following theorem relating monitor slacks δ_i to an upper bound of the aggregate eigen-error ϵ^* [9].

Theorem 1 *Under the above assumptions on filtering errors, setting $\delta_1, \ldots, \delta_n$ to satisfy*

$$2\sqrt{\frac{\bar{\lambda}}{m} \cdot \sum_{i=1}^{n} \sigma_i^2} + \sqrt{\left(\frac{1}{m} + \frac{1}{n}\right) \sum_{i=1}^{n} \sigma_i^4} = \epsilon \qquad (2)$$

guarantees that $\epsilon^* \leq \epsilon$ with probability $\geq 1 - o(\frac{1}{m^3})$.

(We refer to ϵ as *tolerable eigen-error* in what follows.) Similar results can be obtained for eigen-subspaces $\mathbf{C}_a$ and individual eigenvalues [9]. The key idea is to use the aggregate condition in Theorem 1 to determine "good" local monitor slacks δ_i given a tolerable eigen-error ϵ. This requires us to quantify the relationship between error variances σ_i and local slacks δ_i. We now discuss different techniques employed in our system for this purpose.

Homogeneous Slack Allocation: Uniform Distribution Method. A simple method that often works well in practice is to assume that filtering errors are independently and uniformly distributed in $[-\delta_i, \delta_i]$. This gives a closed form for local variances: $\sigma_i = \frac{\delta_i^2}{3}$. Assuming homogeneous slack allocation, that is, all monitors share the same slack $\delta_i = \delta$, we can directly solve Eqn. (2) for δ:

$$\delta = \frac{\sqrt{3\bar{\lambda}n + 3\epsilon\sqrt{m^2 + m \cdot n}} - \sqrt{3\bar{\lambda}n}}{\sqrt{m+n}}$$

Homogeneous Slack Allocation: Local Variance Estimation Method. In some cases, the uniform-distribution assumption for filtering errors may be unrealistic. A more accurate method is to estimate local error variances $\sigma_i(\delta)$ directly from the data, given a choice of δ across all monitors. Variance estimation is performed locally (at each monitor) by fitting a (e.g., quadratic) function of δ using a recent window of observations. These local functions are sent to the coordinator (either periodically or on-demand), and plugged into Eqn. (2) to solve for a new δ. While imposing some additional overhead on the network and local monitors, this method avoids possibly unrealistic uniformity assumptions on the monitor data.

Heterogeneous Slack Allocation. Rather than allocating slack homogeneously across all monitors, a more intelligent solution is to allow for different local slacks $\delta_1, \ldots, \delta_n$ that can dynamically adapt to local stream characteristics. The goal, of course, is to minimize the overall data communication cost subject to the aggregate constraint in Theorem 1. More formally, let the message update frequency (a direct measure of communication cost) of each monitor M_i be a function $f_i(\delta_i)$. Then, using the uniform distribution method as an example, we can formalize heterogeneous slack allocation as the following optimization problem:

$$\text{Minimize} \quad \sum_{i}^{n} f_i(\delta_i) \quad \text{such that} \quad 2\sqrt{\frac{\bar{\lambda}}{m} \cdot \sum_{i=1}^{n} \frac{\delta_i^2}{3}} = \epsilon,$$

where the second summand in Eqn. (2) is ignored, since it is typically an order of magnitude smaller than the first. (A similar formulation can also be given for the local variance estimation method [9].)

As in [18], we can show that the update frequency function has roughly the form $f_i(\delta_i) = z_i \delta_i^{-2}$. Using Lagrange multipliers, we can show that the optimal slack allotments satisfy: $\sum_i^n \delta_i^2 = \frac{3m\epsilon^2}{4\bar{\lambda}}$ and $\frac{f_i}{\delta_i^2}$ = constant. Thus, we aim to allocate slacks δ_i such that the ratios $\frac{f_i}{\delta_i^2}$ are equal across all monitors under an aggregate constraint on δ_i's. The coordinator has information on both f_i and δ_i, and can adaptively allocate monitor slacks using shrinking/growing protocols similar to those in [18].

We have implemented the above techniques in our system and discuss their behavior in practice in Section V.

B. From false alarm deviation to eigen-error

Unfortunately, there is no closed-form solution for determining the tolerable eigen-error ϵ given a desired bound on the false alarm probability $\hat{\alpha}$. We once again follow the inverse dependency path, analyzing the impact of eigen-error ϵ on the deviation $\mu = \hat{\alpha} - \alpha$ of the false alarm probability. The basic idea is that, since the coordinator has access to the filtered data stream $\hat{\mathbf{Y}}$, given eigen-error ϵ, the coordinator can bound the deviation of $\|\hat{\mathbf{C}}_a \hat{\mathbf{y}}\|^2$ and the threshold $\hat{Q}_\alpha$ from their true values. This, in turn, allows us to bound the impact on the detection condition $\|\hat{\mathbf{C}}_a \hat{\mathbf{y}}\|^2 > \hat{Q}_\alpha$ at the coordinator, and, consequently, the change in false alarm probability μ.

Note that μ is typically monotonically increasing in ϵ: larger eigenvalue perturbations naturally imply higher false alarm probabilities. Thus, given an efficient method for computing μ for a given tolerable eigen-error ϵ, our strategy is to determine ϵ for a given μ using a simple *binary search*. Thus, in what follows, we focus on estimating μ given a desired ϵ. Our analysis relies on considering the following random variable:

$$X = \frac{\phi_1[(\|\mathbf{C}_a \mathbf{y}\|^2/\phi_1)^{h_0} - 1 - \phi_2 h_0(h_0 - 1)/\phi_1^2]}{\sqrt{2\phi_2 h_0^2}} \qquad (3)$$

where $h_0 = 1 - \frac{2\phi_1\phi_3}{3\phi_2^2}$, $\phi_p = \sum_{j=k+1}^{n} \lambda_j^p$ for $p = 1, 2, 3$. The X random variable essentially normalizes the random quantity $\|\mathbf{C}_a \mathbf{y}\|^2$ and is known to approximately follow a standard normal distribution [13]. Then, to perform centralized detection on $\|\mathbf{C}_a \mathbf{y}\|^2$ with false alarm α, the threshold Q_α can be determined as a a high-order complex function of $\lambda_{k+1}, \ldots, \lambda_n$ [11]. Based on (3), we can express the false alarm probability (in the centralized case) as

$$\mathbf{Pr}\left[\|\mathbf{C}_a \mathbf{y}\|^2 > Q_\alpha\right] = \mathbf{Pr}\left[X > c_\alpha\right] = \alpha,$$

where c_α denotes the $(1-\alpha)$-percentile of a standard normal distribution.

In our distributed setting, the anomaly detector only has access to the filtered data matrix $\hat{\mathbf{Y}}$, the perturbed statistic $\|\hat{\mathbf{C}}_a \hat{\mathbf{y}}\|^2$, and the perturbed eigenvalues $\hat{\lambda}_{k+1}, \ldots, \hat{\lambda}_n$. As a result, we only observe a perturbed version $\hat{X}$ of the random variable X. Let η_X denote an upper bound on $|\hat{X} - X|$. Then,

```
Procedure FalseAlarmToEigenError($\mu$, err)
Input: Deviation $\mu$ of false alarm probability; desired approximation
        factor (err) for eigen-error $\epsilon$.
1. $\epsilon_l$ := 0.0;  $\epsilon_u$ := $\bar{\lambda}$        // search range for $\epsilon$
2. while ( $(\epsilon_u - \epsilon_l) >$ err $\cdot \epsilon_l$ ) do
3.     $\epsilon$ := $0.5 \cdot (\epsilon_l + \epsilon_u)$
4.     $\eta_X$ := MonteCarloSampling($\epsilon$)
5.     $\mu^*$ := $\mathbf{Pr}\left[c_\alpha - \eta_X < N(0,1) < c_\alpha\right]$
6.     if ($\mu^* > \mu$) then $\epsilon_u$ := $\epsilon$ else $\epsilon_l$ := $\epsilon$
7. return($\epsilon$)
```

Fig. 5. Procedure for estimating eigen-error given a false alarm probability deviation μ using binary search.

the deviation of the false alarm probability in our distributed detection scheme can be approximated as

$$\mu = \mathbf{Pr}\left[c_\alpha - \eta_X < N(0,1) < c_\alpha\right] \tag{4}$$

where $N(0,1)$ denotes a standard normal random variable. A key issue here is how to estimate the η_X upper bound on $|\hat{X} - X|$. Our approach is to use a *Monte Carlo (MC) sampling* technique to obtain observations of the $|\hat{X} - X|$ random variable, and use the maximum of these observations as an estimate of η_X. (Due to space constraints, the details can be found in [9].) A pseudo-code description of our method for estimating the eigen-error ϵ corresponding to a desired μ is given in Fig. 5.

V. Evaluation

A. Evaluation Methodology and Metrics

We implemented our system and developed a trace-driven simulator to validate our methods. The real world traffic, used as input to our simulator, comes from the Abilene network. We used four one-week traces of router-to-router origin-destination (OD) traffic matrices. The traces contains OD-flow traffic loads measured every 10 minutes, for all 121 flows of the Abilene network, from which we can compute the per-link traffic loads for all 41 links, using its provided routing matrix. With a time unit of 10 minutes, data was collected for 1008 time units for each week.

To evaluate the detection accuracy of our approach, we synthetically injected 60 anomalies and 60 non-malicious bursts [4] into the dataset using the method described in [15], so that we would have sufficient anomaly data to compute error rates. We used a threshold Q_α corresponding to an $1-\alpha = 99.5\%$ confidence level. In the detection process, when any anomaly is missed, we count it as a missed detection; when any non-malicious burst is detected, we count it as a false alarm. To make the results intuitive, we define the *false alarm rate* as the fraction of false alarms over the total number of injected bursts, which is α (defined in Sec. III) re-scaled as a rate rather than a probability. We define *missed detection rate* as the fraction of missed detections over the total number of injected anomalies.

[4]In [15] the authors use the term "small anomaly" to refer to events that should be ignored (not flagged) and whose detection counts as false alarms. While we use their same method for synthetic anomalies, we change the terminology to be more intuitive.

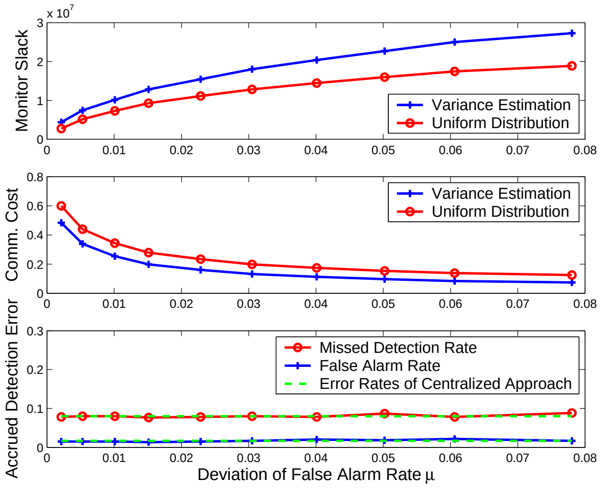

Fig. 6. Monitor slacks, communication cost and accrued detection. The dashed line is the detection error of centralized approach with complete data.

In order to evaluate the scalability of our method, we had to generate synthetic traffic matrices because no traffic matrix datasets with thousands of links and tens of thousands of OD flows exist. We used the BRITE topology generator [3] to generate both sample topologies and their associated routing matrices. We considered a number of networks with anywhere from 100 to 1000 links, and up to 500×500 pairs of OD flows. For each of the $250,000$ OD flows, we generate four weeks of data based on the method discussed in [17], by extracting the relevant statistics (e.g., mean distribution, noise level, etc.) from the Abilene network traffic matrices.

We compute the communication cost as follows. Let num be the number of messages exchanged between monitors and the coordinator, including both the signal updates from monitors to coordinator as well as the slack updates from the coordinator to the monitors. Let n be the number of monitors and m the number of values in each monitor's time series. Then communication cost is calculated as $num/(n \cdot m)$ which gives the per-monitor communication cost.

B. Detection accuracy vs. communication cost

We now evaluate the performance and tradeoffs of our protocols and algorithm for computing the monitor slacks. We implemented both methods of homogeneous allocation for computing the monitor slack δ: the closed-form solution relying on uniform assumptions and the variance measurement solution.

In Fig. 6 we consider a whole range of possible inputs on the tolerable false alarm rate deviation μ (the probability Eqn (4)is re-scaled to a rate). We show in the top plot the relationship between μ and the filtering slack δ, in the middle plot the relationship between μ and communication cost. These results make intuitive sense. As we allow more error tolerance μ, we can use greater slack and filter out more data at the

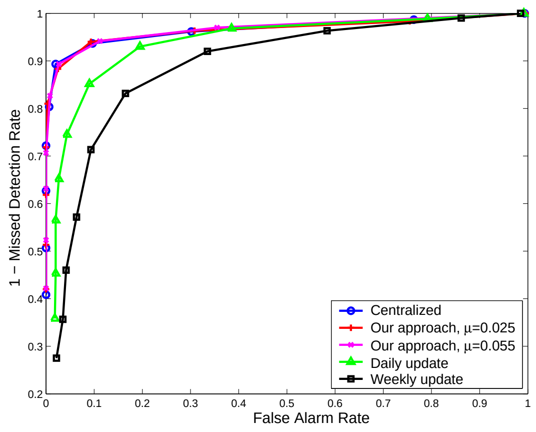

Approach	Communication Cost
Centralized, daily and weekly update	1.000
Our approach, $\mu = 0.025$	0.159
Our approach, $\mu = 0.055$	0.097

Fig. 7. ROC curve: benefit and cost of data update approaches.

monitors, and consequently reduce the amount of data sent to the coordinator over the network. For example, when the tolerable deviation of false alarm is 5%, our algorithm reduces the data sent through the network by more than 90% when using the variance estimation method.

The bottom plot shows the actual accrued detection errors. The curve with circles depicts the missed detection rate; the curve with pluses depicts the false alarm rate; the dashed lines depict the corresponding detection errors of the centralized approach. First we point out that in all cases, the the actual false alarm rate with our protocols is always smaller than the guaranteed bound. In other words, although we may input that we can tolerate an additional μ = 5% errors, in fact we don't have to incur this reduced performance, because the lower plot illustrates that our method performs nearly identically to the original subspace method in terms of false alarms and missed detections. Moreover, this nearly identical error performance can be achieved with far less data; values such as 80% or 90% less data (depending upon the particular value of μ) are typical. These results illustrate, that for our dataset, the reduction in communication costs can be enormous whereas the tradeoff in terms of increased error performance is very small. These promising results confirm our hypothesis that it is not necessary to back-haul all the data for an anomaly detection such as [15].

In comparing the variance estimation and the uniform distribution methods for slack estimation, we see that the measurement based variance estimation method always performs better. The absolute difference in communication cost varied from 5% to 10% for tight requirements on μ (with μ=0.006 to 0.08, respectively). The advantage of the closed-form method is its simplicity and low computational overhead. Since, for this dataset, its performance is quite close to the measurement-based method, we conclude that such solutions might be ”good enough” for many datasets.

We now compare our method and the original subspace method using an ROC curve [22]. The y-axis plots the true positives (one minus the missed detections) and the x-axis depicts the false alarms. ROC curves allow one to compare two methods over a range of detection thresholds; each point on each curve corresponds to a different cutoff threshold for signaling an alarm. In general, if one curve lies entirely above and left of another [22], then that method is superior in that it handles the tradeoff between missed detections and false alarms better.

Because in [15] they do not indicate how often they update their PCA transform, we tested 3 variants of their method. The ”centralized” version updates the principle components each time interval (upon the arrival of new data). The ”daily update” version updates the principle components once a day (based on the previous 24 hours); the ”weekly update” version updates the components once a week (based on the previous week). The results are shown in Fig. 7.

We can see from the plot that the ROC curve and detection accuracy of our distributed online approach (either $\mu = 0.015$ or $\mu = 0.045$) are fairly close to that of the centralized approach. This is interesting and rather surprising: it means that our use of filtered data almost does not inject any bias into the statistical tension between the underlying distributions of normal and abnormal signals. Using 10% to 20% of original data, our distributed online approach can keep the projection matrix and the threshold up-to-date and has a detection ability that is essentially as good as the fully centralized approach.

It does appear to be important to keep the principle components up to date because the performance drop-off is considerable for either the daily or weekly data update cases. This indicates that our ideas geared towards keeping the principle components (as well as the projection matrix and cutoff threshold) up to date are important. We remind the reader that we allow the principle components to be kept up to date less intensively than the original method for two reasons: there are some time intervals when no data is sent and thus no update is required, and we use the low-rank update algorithm. Both of these factors reduce the computation overhead at the coordinator. We point out that there may be additional ways to reduce this computation overhead such as checking the norm of the covariance matrix and only doing updates if the change to this norm ”is large enough”. We leave that for future work.

We also implemented our heterogeneous slack allocation and compared its performance to that of the homogeneous slack allocation. We found that the performance did not differ greatly (at most 3% in terms of communication costs) between the two. This indicates that the simpler solution may be good enough for the data type we consider. However the benefits of having the more general solution using heterogeneous slacks would need to be evaluated for each data type and application.

C. System Scalability

We now examine our system's scalability as the number of distributed monitors grows. Recall that one of the key reasons for controlling the communications cost is to avoid overwhelming the coordinator should it receive lots of data from many monitors. The communications cost metric we have

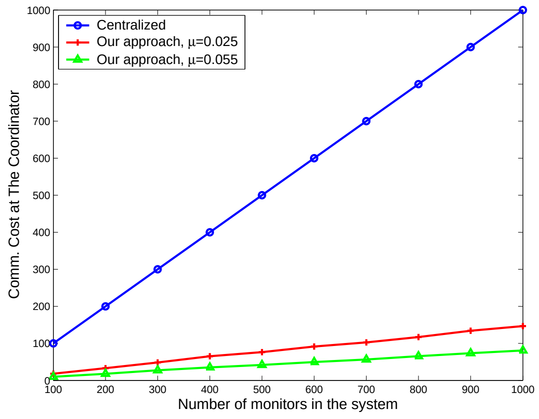

Fig. 8. System Scalability.

been using until now (namely $num/n \cdot m$) is an average value for the cost *per monitor*. The communication cost coming into the coordinator is the sum of costs of all monitors, which is can be computed from num/m. This captures the average number of messages the coordinator receives in one time slot.

We plot the communications cost at the coordinator as a function of the number of monitors in Fig. 8. We varied the number of monitors from 100 to 1000, and used tolerable deviation of false alarm rate $\mu = 0.025$ and $\mu = 0.055$. For each system size n, we run 5 rounds of experiments, each of which runs on n randomly picked monitors. In the Figure, in our approach, as the system size increases: 1) the communication cost of each monitor roughly keeps constant (which is the slope of the line); and 2) the communication cost at coordinator increases linearly with system size with the slope roughly being 0.150 ($\mu = 0.025$) and 0.088 ($\mu = 0.055$), which are far less than 1.0, the slope of the centralized approach. This result indicates that the communication cost increases slowly as system size increases, and that our system thus scales gracefully.

VI. Conclusion

In this paper we extended the PCA-based anomaly detection method using ideas from ”in-network” processing (to engage local monitors to filter based on global conditions) combined with ideas from stochastic matrix perturbation theory. Perturbation theory is used to derive bounds on the terms in the anomaly detector that are affected by error propagation when limited data is used. We designed an algorithm to select filtering parameters so that that monitors only send data to the central tracking site ”when necessary”. The necessity is determined from individual traffic behaviors, correlations across traffic streams and the global trigger tracking condition. We show that anomaly detection can still be done very accurately even when 80 or 90% of the original data is never sent to the coordinator. Thus the tradeoff between detection accuracy and communication savings is very lopsided - there is a huge reduction in communication overhead accompanied by a very small increase in errors. Moreover we illustrated that this data reduction leads to a system that scales gracefully as the number of monitors grows. In particular, we showed that the coordinator's input data rate grows more than an order of magnitude more slowly than a system that back-hauls all monitoring data for volume anomaly detection.

References

[1] Barford, P., Kline, J., Plonka, D., and Ron. A. A signal analysis of network traffic anomalies. In *IMW* (2002).

[2] Brand, M. Fast low-rank modifications of the thin singular value decomposition. In *Linear Algebra and Its Applications*, 415(1) (2006)

[3] Medina, A., Lakhina, A., Matta, I. and Byers, J. BRITE: an approach to universal topology generation. In *MASCOTS* (2001).

[4] Brutlag, J. Aberrant Behavior Detection in Timeseries for Network Monitoring. In *LISA* (2000).

[5] Cormode, G., and Garofalakis, M. Sketching streams through the net: Distributed approximate query tracking. In *VLDB* (2005).

[6] Dilman, M., and Raz, D. Efficient reactive monitoring. In *IEEE INFOCOM* (2001).

[7] DRMAC, Z. On principal angles between subspaces of euclidean of space In *SIAM J. Matrix Anal. Appl.*, 22(1) 2000.

[8] Huang, L., Nguyen, X. L., Garofalakis, M., Jordan, M., Joseph, A.D., and Taft, N. Distributed PCA and network anomaly detection. (Submitted to NIPS 2006).

[9] Huang, L., Nguyen, X. L., Garofalakis, M., Hellerstein, J., Jordan, M., Joseph, A.D., and Taft, N. Communication-efficient online detection of network-wide anomalies. UCB Technical Report, August 2006.

[10] Huebsch, R., and et al. Querying the internet with pier. In *VLDB* (2003).

[11] Jackson, J. E. and Mudholkar, G. S. Control procedures for residuals associated with principal component analysis. In *Technometrics*, pages 341-349, 1979.

[12] Jain, A., Chang, E. Y., and Wang, Y.-F. Adaptive stream resource management using kalman filters. In *ACM SIGMOD* (2004).

[13] Jensen, D. R. and Solomon, H. A Gaussian approximation for the distribution of definite quadratic forms. In *J. Amer. Stat. Assoc.*, 67(1972), 898-902.

[14] Keralapura, R., Cormode, G., and Ramamirtham, J. Communication-efficient distributed monitoring of thresholded counts. To appear in *ACM SIGMOD* (2006).

[15] Lakhina, A., Crovella, M., and Diot, C. Diagnosing network-wide traffic anomalies. In *ACM SIGCOMM* (2004).

[16] Lakhina, A., Papagiannaki, K., Crovella, M., Diot, C., Kolaczyk, E. D. and Taft, N. Structural analysis of network traffic flows. In *ACM SIGMETRICS*, (2004).

[17] Nucci, A., Sridharan, A. and Taft, N. The problem of synthetically generating IP traffic matrices: initial recommendations. In *ACM CCR*, July 2005

[18] Olston, C., Jiang, J., and Widom, J. Adaptive filters for continuous queries over distributed data streams. In *ACM SIGMOD* (2003).

[19] Padmanabhan, V. N., Ramabhadran, S., and Padhye, J. Netprofiler: Profiling wide-area networks using peer cooperation. In *IPTPS* (2005).

[20] Renesse, R. V., Birman, K., and Vogels, W. Astrolabe: a robust and scalable technology for distributed system monitoring, management and data mining. *ACM Trans. on Computer Systems*, 21(2) (2003).

[21] Sharfman, I., Schuster, A. and Keren, D. A geometric approach to monitoring threshold functions over distributed data streams In *ACM SIGMOD* (2006).

[22] Soule, A., Salamatian, K., and Taft, N. Combining filtering and statistical methods for anomaly detection. In *IMC* (2005).

[23] Spring, N., Wetherall, D., and Anderson, T. Scriptroute: A facility for distributed internet measurement. In *USITS* (2003).

[24] Stewart, G. W., and Sun, J.-G. *Matrix Perturbation Theory*. Academic Press, 1990.

[25] Xie, Y., Kim, H.-A., O'Hallaron, D. R., Reiter, M. K., and Zhang, H. Seurat: A pointillist approach to anomaly detection. In *RAID* (2004).

[26] Yegneswaran, V., Barford, P., and Jha, S. Global intrusion detection in the domino overlay system. In *NDSS* (2004).

[27] Zhang, Y., Ge, Z.-H., Greenberg, A., and Roughan, M. Network anomography. In *IMC* (2005).

[28] Zhao, B., Huang, L., Stribling, J., Joseph, A., and Kubiatowicz, J. Exploiting Routing Redundancy via Structured Peer-to-Peer Overlays. In *IEEE ICNP* (2003).